

Chemical deterioration of Al film prepared on CF₄ plasma-etched LiNbO₃ surface

Hirotohi Nagata,^{a)} Yasuyuki Miyama, and Naoki Mitsugi

Optoelectronics Research Division, New Technology Research Laboratories, Sumitomo Osaka Cement Co., Ltd., 585 Toyotomi-cho, Funabashi-shi, Chiba 274-8601, Japan

Kaori Shima

Advanced Materials Research Division, New Technology Research Laboratories, Sumitomo Osaka Cement Co., Ltd., 585 Toyotomi-cho, Funabashi-shi, Chiba 274-8601, Japan

(Received 30 August 1999; accepted 23 November 1999)

The fabrication process of an Al thin-film optical polarizer on LiNbO₃ waveguides after CF₄ plasma dry etching of a previously deposited SiO₂ buffer layer was investigated. The problem in this process is a precipitation of compounds containing C, O, F, and Li on the etched LiNbO₃ surface and a chemical deterioration of the Al caused by a reaction with these precipitates. Most notably, the growth of amorphous phase in addition to the crystalline Al metal grains and a partial oxidization of Al were found at the interface using transmission electron microscopy and x-ray photoelectron spectroscopy.

I. INTRODUCTION

The demand for LiNbO₃ integrated optical waveguide devices has rapidly increased in order to realize the needs of high-speed communication systems. In this regard, processes unusual for LiNbO₃ are sometimes attempted to improve the device performance.^{1,2} Plasma dry etching of the wafer surface is one of these uncommon processes, although it is a common process for semiconductor devices. Concerning dry etching of LiNbO₃, we know of only a few reports on preparation of ridgelike waveguides on LiNbO₃ by reactive ion etching (RIE) or by electron cyclotron resonance (ECR) plasma etching.^{3,4} Recently, we also have investigated the ECR etching of LiNbO₃ surface with CF₄ and CHF₃ and found fluorination of the surface, a precipitation of LiF, and fluorocarbons.^{5,6} These fluoride precipitates were found to cause a weakening of bonding strength of the SiO₂ buffer layer which was deposited on the etched LiNbO₃ surfaces.⁷ We examine here another undesirable effect of the fluoride precipitates on CF₄ plasma etched LiNbO₃ surface in device fabrication processes.

For instance, in x-cut LiNbO₃ waveguide modulator devices, one can integrate an optical polarizer by depositing Al metal film on the Ti:LiNbO₃ waveguides, which selectively propagates extraordinary light.⁸ On the other hand, a high-speed modulator needs a thick SiO₂ buffer layer between waveguides and corresponding electrodes to adjust

the speed of microwaves propagating in the electrode. Because the SiO₂ layer is annealed in O₂ at higher temperatures after its deposition, the Al thin-film polarizer must be prepared after removing a part of the annealed SiO₂ layer on the waveguide. As a method to make a window in the SiO₂ film for direct Al deposition onto the LiNbO₃ waveguide, a conventional plasma-etching technique using fluorocarbons seems to be effective. In this report, we investigated problems occurring in the process consisting of CF₄ plasma etching of the SiO₂ film on LiNbO₃ and deposition of the Al metal film on the exposed LiNbO₃ surface.

From the viewpoint of device performance, sometimes the Al thin-film polarizer prepared by the above process did not work well. The surface of the failed Al film was not metallic and chemical deterioration of the film at the interface was suspected. The precipitates on the etched LiNbO₃ were thought to be a plausible cause for the deterioration of Al films.

II. EXPERIMENTAL PROCEDURE

On a commercial x-cut LiNbO₃ wafer without waveguides, about 600-nm-thick SiO₂ film was prepared by vacuum evaporation deposition followed by O₂ annealing at 600°C for 5h. In some experiments, a sputter-deposited SiO₂ film on the LiNbO₃ was used for comparison. Etching of the SiO₂ layer was carried out in an ECR plasma-etching machine using CF₄ as an etching gas at ambient temperature. A typical etching condition is a gas pressure of 0.02 Pa, a microwave power of 400 W, an acceleration electrode voltage of 500 V, and a gap distance of 200 mm between the electrode

^{a)} e-mail: hinagata@sits.soc.co.jp

and the sample. A plasma gas monitor (ULVAC: REPROSS RE202P, Tokyo) consisting mainly of a turbo molecular pump and a mass spectrometer was installed on the etching chamber to check the end point of SiO₂ etching. About 100-nm-thick Al thin films were deposited on both virgin and etched SiO₂/LiNbO₃ surfaces by conventional direct current (dc) sputtering of an Al target with Ar.

Examination of the Al/LiNbO₃ interface was carried out by Auger electron spectroscopy (AES), x-ray photoelectron spectroscopy (XPS) with Al K_α radiation, secondary ion mass spectroscopy (SIMS) with Cs⁺ and O₂⁺ ion beams, and transmission electron microscopy (TEM). Further, the etched surface before the Al film deposition was examined by atomic force microscopy (AFM).

III. RESULTS AND DISCUSSION

A. Dry-etching process of SiO₂ on LiNbO₃

Figure 1 shows etching time dependency of various gas fragments existing in the etching chamber [Fig. 1(a)] and obtained etching depth [Fig. 1(b)]. The gas fragments for *in situ* plasma monitoring corresponded to mass numbers of 20, 28, 31, 50, and 85. Considering that the SiO₂ layer including hydroxyl impurities was etched by CF₄ plasma, the peaks might be assigned as #20 for HF, #28 for CO, #31 for CF, #50 for CF₂, and #85 for SiF₃. As is seen, the intensity profile of these peaks showed a steplike change after 1000 s of etching; the peaks of #28 (HF) and #85 (SiF₃) weakened and the other peaks increased slightly. This specific point

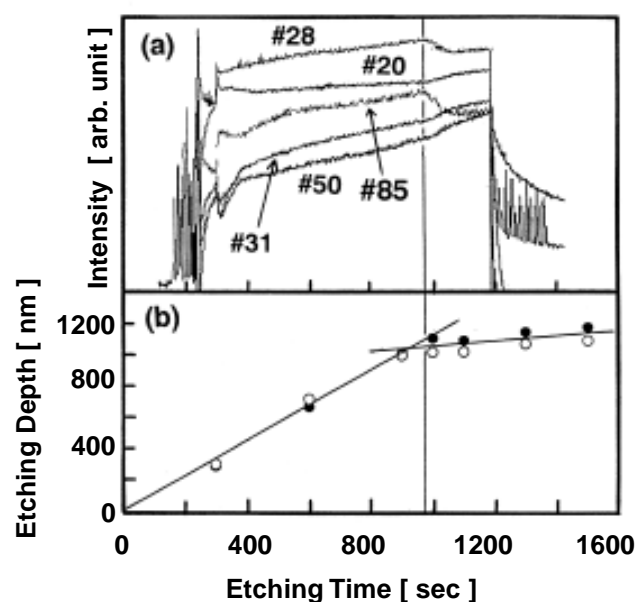


FIG.1. Etching time dependency of (a) various gas fragments existing in the etching chamber and (b) obtained etching depth. The numbers in (a) denote mass numbers: #20 for HF, #28 for CO, #31 for CF, #50 for CF₂, and #85 for SiF₃. Open circles and closed circles in (b) denote etching results for vacuum-evaporation-deposited SiO₂ and sputter-deposited SiO₂, respectively.

was found to correspond to the time at which the measured etching rate slowed, as shown in Fig. 1(b). In Fig. 1(b), the etched depths for the vacuum evaporation deposited SiO₂ (open circles) and the sputtering deposited SiO₂ (closed circles) were plotted, and the etching rate (slope of the line) decreased beyond 1000 s. The etching depth was measured by a stylus method after interrupting the etching. Because the point at which the etching rate decreased abruptly is expected to be the interface between SiO₂ layer and LiNbO₃ substrate, the intensity reduction of the mass peak #85 (probably from SiF₃) at the same point may indicate that the SiO₂ layer was removed almost completely and the LiNbO₃ surface appeared.

In order to check the appearance of the LiNbO₃ surface, the etching was stopped at a certain time and the etched surface was examined by an AES analyzer. Figure 2 shows changes in the AES profile depending on the etching time. The etching time, denoted by lines (a)-(e), was selected by monitoring the changes of the mass peak intensity of #85, as schematically shown in Fig.2. At time (b), the mass peak intensity commenced to decrease until time (d). The fact that an Auger electron peak due to Nb appeared at time (b)

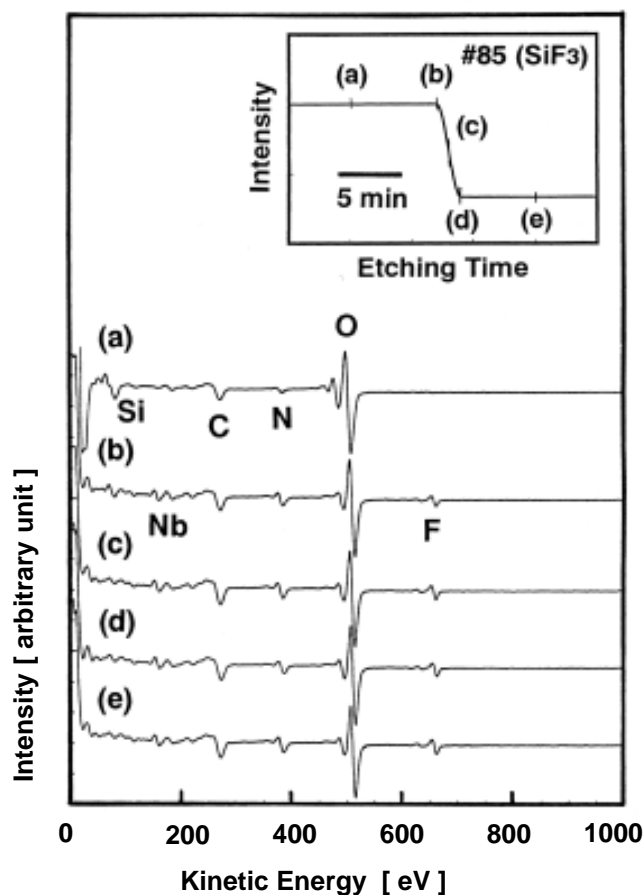


FIG. 2. AES profiles measured on SiO₂/LiNbO₃ samples after various etching time. The etching time, denoted by (a)-(e), was determined by monitoring the changes of the mass peak intensity of #85 (SiF₃).

suggested that the steplike reduction of the #85 mass peak intensity showed the appearance of the LiNbO₃ surface. After the appearance of LiNbO₃, an existence of F on the etched surface was found as shown by the AES profiles (b)-(e). This is consistent with results of our previous investigation on ECR plasma etching of LiNbO₃, in which the precipitation of particles consisting of LiF and fluorocarbon polymers was observed on the etched surface.^{5,6}

Figure 3 shows AFM images of the etched surfaces (1 × 1 μm area); SiO₂ layer [Fig. 3(a)], SiO₂/LiNbO₃ interface [Fig. 3(b)], and LiNbO₃ substrate [Fig. 3(c)]. The surface roughness *Ra* of the etched SiO₂ layer [Fig. 3(a)] was about 1 nm and was similar to that before the etching. After the appearance of LiNbO₃ [Figs. 3(b) and 3(c)], however, the surface was roughened to be in an order of *Ra* = 10 nm, although a typical surface roughness of the virgin LiNbO₃ substrate was *Ra* = 2 nm. Judging from the above AES and AFM results, we consider that even after the SiO₂ layer was etched out completely, the LiNbO₃ crystal surface was recoated with materials generated by the chemical reaction of CF₄ plasma with LiNbO₃.

B. Interface analyses of Al film on etched LiNbO₃

The color of the Al film on the etched SiO₂/LiNbO₃ was observed to be black at the interface with the LiNbO₃ substrate, while the Al film surface was metallic. Some samples were black throughout the film. On the other hand, the Al films deposited on SiO₂/LiNbO₃ and LiNbO₃ without etching were completely metallic. Thus, chemical reaction at the Al/etched-LiNbO₃ interface was suspected and examined by SIMS, XPS, and TEM.

Figures 4 and 5 show SIMS results for the Al film on SiO₂/LiNbO₃ without etching and the Al film on CF₄ etched SiO₂/LiNbO₃, respectively. An O₂⁺ ion beam was used for analyses of Li and Nb (area size = 75 × 120 μm) and a Cs⁺ beam (120 × 192 μm) for others. The concentrations of H, O, C, and Si were quantitatively measured and plotted in Figs. 4(a) and 5(a), while Li, F, Al, and Nb were shown by the detected peak intensity in Figs. 4(b) and 5(b). The vertical axes of Figs. 4(a) and 5(a) were calibrated by other measurement results on a reference Al sample, in which H, C, O, Si, and Ti ions had been quantitatively implanted. As is seen, the Al film on SiO₂/LiNbO₃ (Fig. 4) was expected to have a sharp interface, although the source of F contaminant in the film was not known. The slight increase in Li and Nb at the Al/SiO₂ interface of Fig. 4 was considered to be due to a diffusion from LiNbO₃ during the SiO₂ film deposition process, judging from results of our previous investigation on SiO₂/LiNbO₃ interface.^{9,10} On the other hand, because the substrate (LiNbO₃) surface was roughened by the etching, the interface profile of the Al film on etched SiO₂/LiNbO₃ was seen to be broad (Fig. 5). However, the amounts

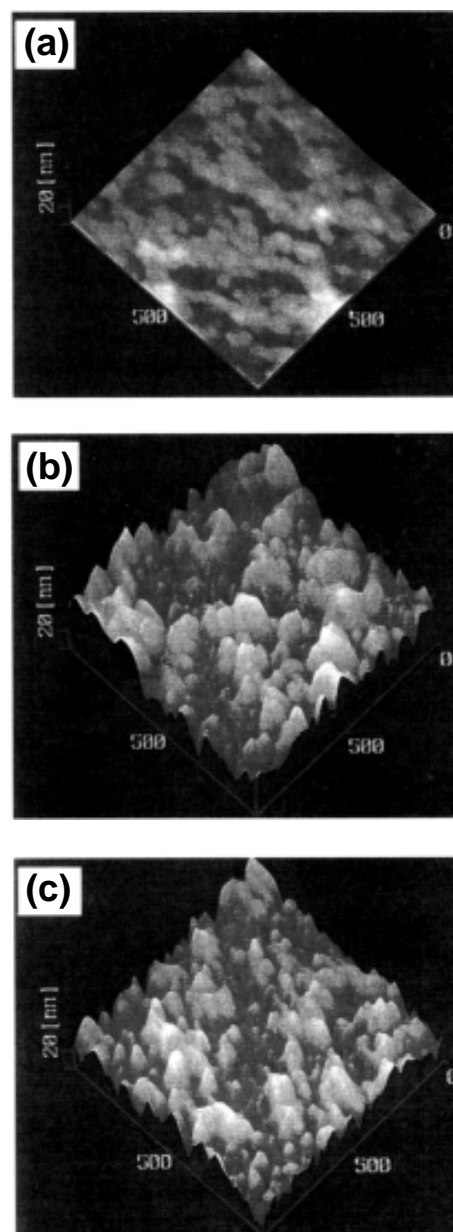
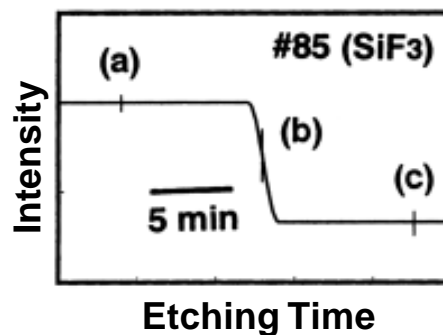


FIG. 3. AFM images of the etched surface (1 × 1 μm area): (a) SiO₂ layer, (b) SiO₂/LiNbO₃ interface, and (c) LiNbO₃ substrate. The etching time, denoted by (a)-(c), was determined by monitoring the changes of the mass peak intensity of #85 (SiF₃).

of F and C seemed to be constant throughout the film and are higher than those in the Al on unetched substrate. The origin of the F and C was thought to be the precipitates consisting of LiF and fluorocarbons, which had been deposited on the LiNbO₃ surface during the prior CF₄ plasma etching.

Figures 6 and 7 reveal XPS analysis results of the Al film samples on the SiO₂/LiNbO₃ and the CF₄ etched SiO₂/LiNbO₃ substrates, respectively. From both samples, photoelectron peaks of C, O, F, Al, and Si were detected. The analysis area was 100 x 100 μm. In these measurements, we focused on the chemical state of Al and examined a chemi-

cal shift of the Al 2p peak. The observed peak consisted of the main peak at 73 eV (bonding energy) and a broad peak around 75 eV. The main peak and the additional broad peak could be assigned to metallic Al and oxidized Al, respectively. We attempted to estimate the amount of oxidized Al by a subtraction of the ideal peak for metallic Al including its peak tailing toward lower energy side from the observed peak. The broad peak left around 75 eV was considered to be the peak for oxidized Al. Thus, the ratio of the two Al phases to total detected Al was calculated from the obtained Al 2p peaks and plotted in Figs. 6 and 7 by white circles for

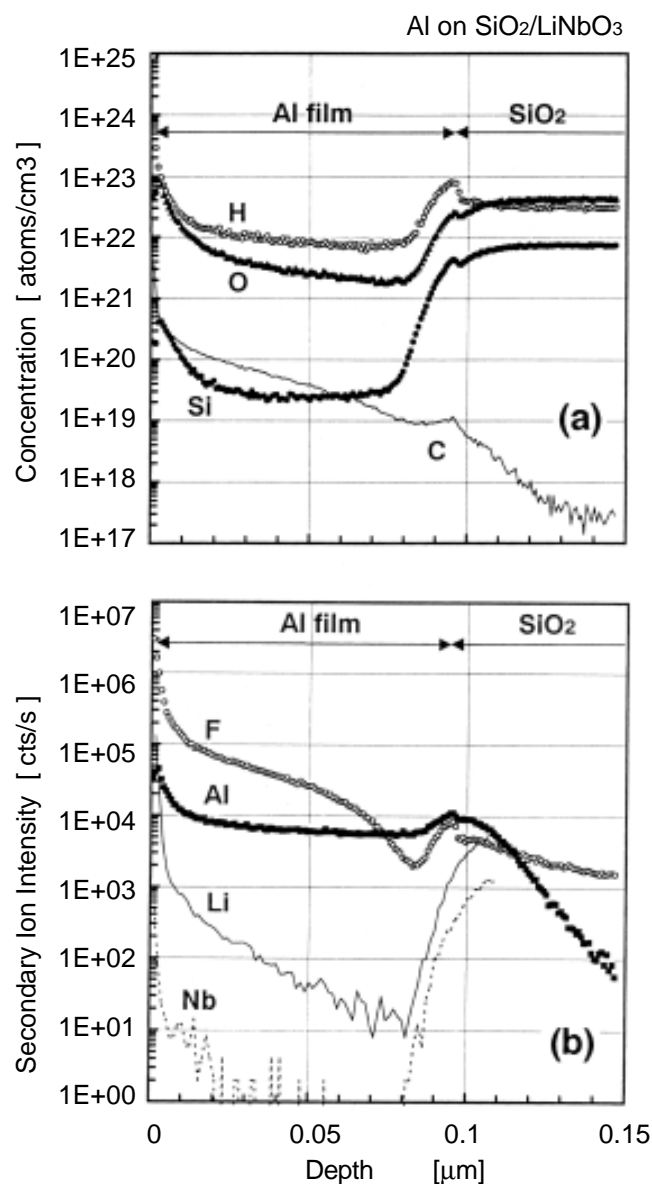


FIG. 4. SIMS results for the Al film on SiO₂/LiNbO₃ without etching. Concentrations of H, O, C, and Si were quantitatively measured and plotted in (a), while Li, F, Al, and Nb were shown by the detected peak intensity in (b).

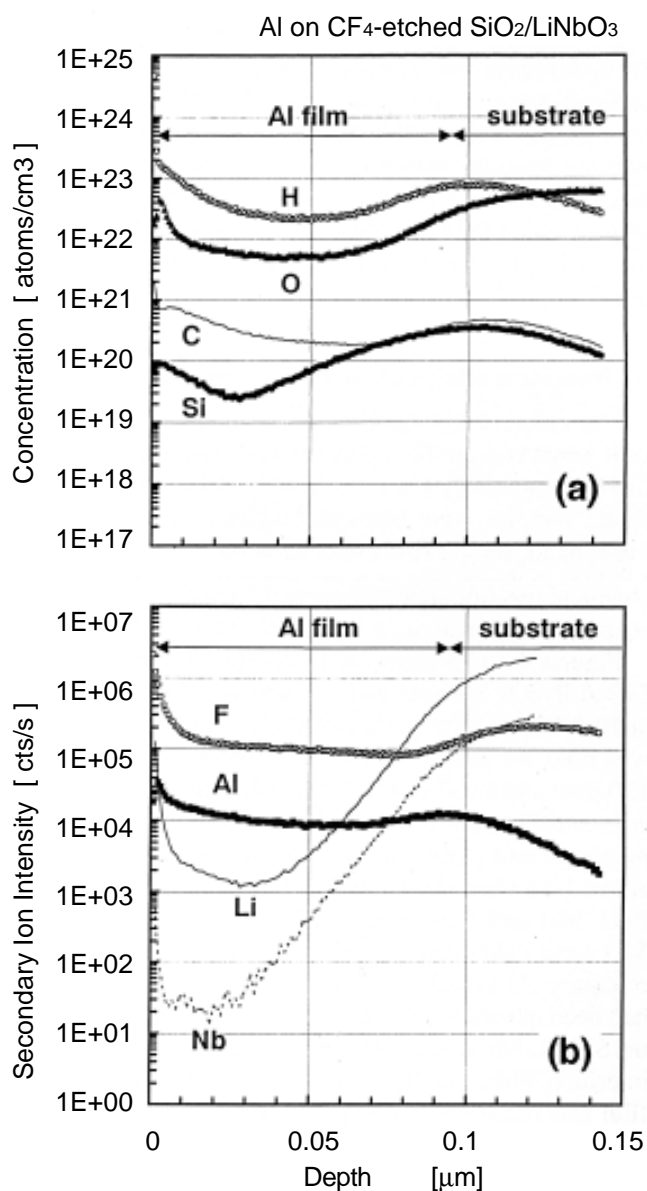


FIG. 5. SIMS results for the Al film on CF₄ plasma-etched SiO₂/LiNbO₃. Concentrations of H, O, C, and Si were quantitatively measured and plotted in (a), while Li, F, Al, and Nb were shown by the detected peak intensity in (b).

metallic Al and black circles for oxidized Al. The chemical state of Al film on the unetched SiO₂/LiNbO₃ was almost completely metallic except for the surface and interface. For

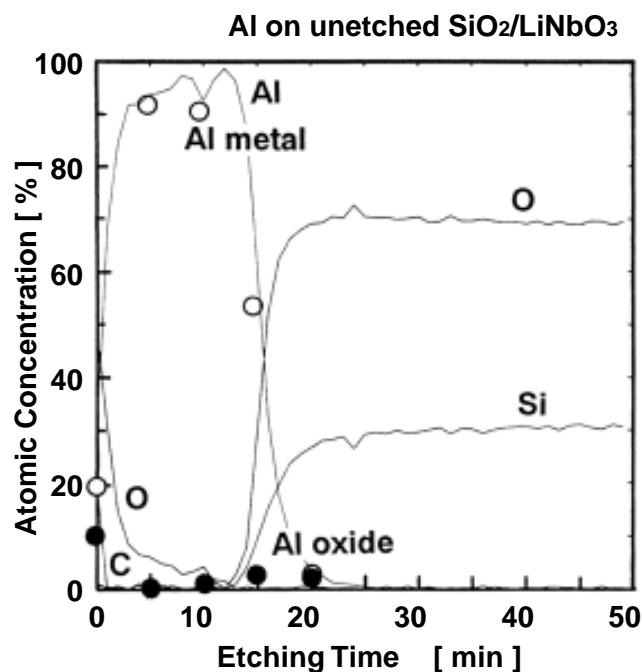


FIG. 6. XPS analysis results for the Al film on unetched SiO₂/LiNbO₃. The ratio of metallic Al (Al 2*p* at 73 eV) and oxidized Al (Al 2*p* at 75 eV) to total detected Al is shown by open and closed circles, respectively.

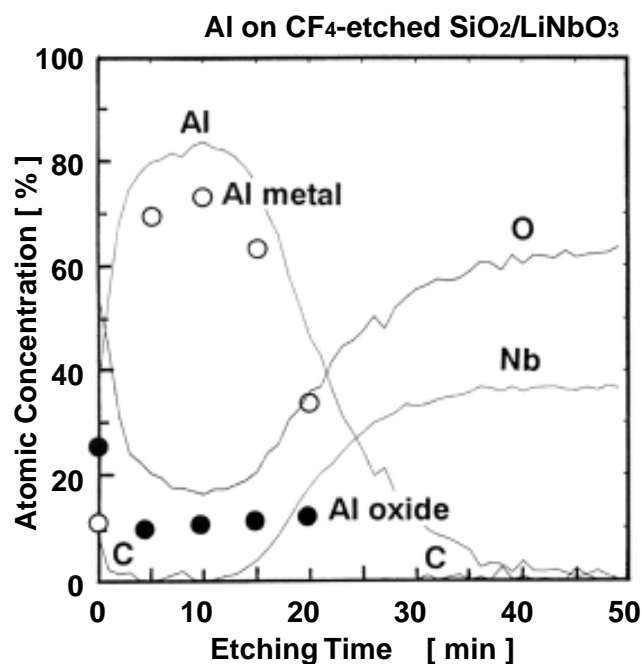


FIG. 7. XPS analysis results for the CF₄ plasma-etched SiO₂/LiNbO₃ substrate. The ratio of metallic Al (Al 2*p* at 73 eV) and oxidized Al (Al 2*p* at 75 eV) to total detected Al is shown by open and closed circles, respectively.

the Al film on the etched SiO₂/LiNbO₃, however, the oxidized Al phase was found to exist even inside the film. The ratio of this oxidized Al was about 13% of the detected Al, as shown in Fig. 7. The results suggest that the Al film on the etched SiO₂/LiNbO₃ was chemically deteriorated due to the interface reaction.

Finally, the physical structure of the Al film on the etched SiO₂/LiNbO₃ was examined by cross-sectional TEM observation. Figure 8 shows the obtained cross-sectional image, in which the dark contrast region is LiNbO₃ substrate and the light contrast region corresponds to the Al film. The electron-diffraction pattern for the Al film region was analyzed and indicated an absence of the preference orientation of the crystalline Al phase. The interface of Al and etched LiNbO₃ was found to be very rough; a peak-to-peak roughness was measured to be about 100 nm. However, the Al film surface was observed to be smoother, although the film thickness varied largely from 50 to 150 nm depending on the roughened interface.

As a reason for the above-observed inconsistency in surface roughness, we consider the following process mainly caused by etching-reaction-induced precipitates on the etched LiNbO₃ surface. As found by TEM images of Fig. 8, the etching edge of the crystalline LiNbO₃ was considered

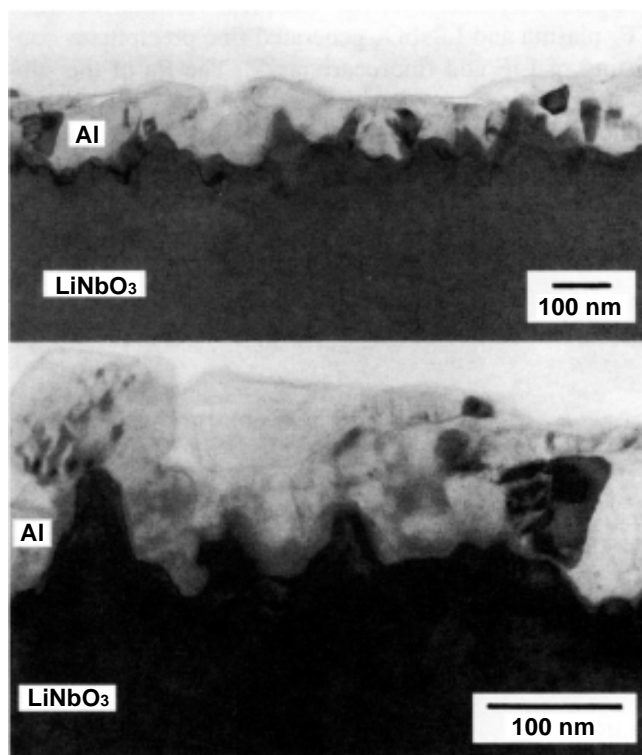


FIG. 8. Cross-sectional TEM images. The dark-contrast region is LiNbO₃ substrate and the light-contrast region corresponds to the Al film.

to be extremely roughened by the etching. Simultaneously, the etching reaction might deteriorate a top surface of the crystal and generated the precipitates on the substrate surface. These reaction-induced layers were suspected to cover the intrinsically roughened crystal surface and make the apparent surface to be smoother as $R_a = 10$ nm. Thus, the Al film deposited on the precipitates layer was thought to have the similarly smooth surface. On the other hand, at the interface of Al film on the substrate, the top layers of the substrate might chemically combine with Al and left the rough edge ($R_a = 100$ nm) of crystalline LiNbO₃, as shown in Fig. 8.

Figure 9 is magnified TEM images of a typical Al film cross section. The film is composed of grains 30 to 100 nm in size, and the existence of amorphous phase was found between grains. Considering SIMS (Fig. 5) and XPS (Fig. 7) results, the amorphous region is expected to be Al compounds such as oxidized Al.

C. Process of Al film deterioration

The above description of Al film deposition on CF₄ plasma etched SiO₂/LiNbO₃ is schematically summarized in Fig. 10. The surface roughness of the SiO₂ film deposited on the LiNbO₃ single crystal substrate by a vacuum evaporation technique was $R_a = 1$ nm [Fig.10(a)]. The plasma etching using CF₄ could remove the SiO₂ surface uniformly keeping the surface smooth [Fig. 10(b)]. However, when the etching reached the SiO₂/LiNbO₃ interface, the chemical reaction between CF₄ plasma and LiNbO₃ generated fine precipitates consisting of LiF and fluorocarbons.⁵⁻⁷ The R_a of the substrate surface covered with the precipitates was 10 nm, although the actual surface of LiNbO₃ crystal was further

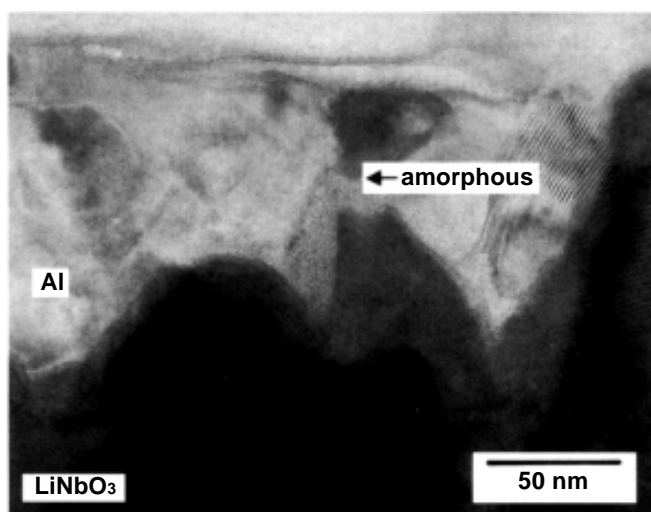


FIG. 9. Magnified cross-sectional TEM image. The dark-contrast region is LiNbO₃ substrate and the light-contrast region corresponds to the Al film.

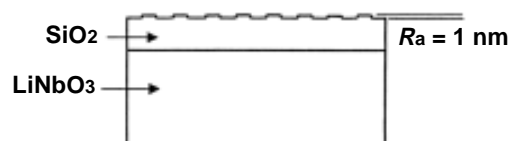
roughened to be $R_{p-p} = 100$ nm due to the etching reaction [Fig. 10(c)]. Because the Al film was deposited on the precipitate layer, the film has a smooth surface [Fig. 10(d)]. However, the precipitates on LiNbO₃ are expected to be chemically reactive and provided O, F, C, Li contaminant elements into the Al film. The chemical reaction at the interface caused a growth of amorphous compounds such as oxidized Al in the polycrystalline Al film [Fig. 10(e)].

In order to prepare an optical polarizer on LiNbO₃ waveguides, the deposited Al film must be metallic to partially absorb the propagating light. In this regard, the fabrication procedure examined here, including plasma dry-etching process of the substrate, is thought to result in incomplete growth of metallic Al.

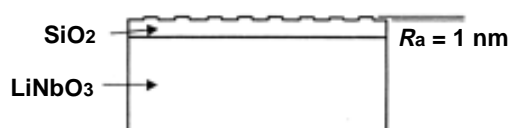
IV. CONCLUSION

The chemical reaction at the interface of Al film on CF₄ plasma-etched SiO₂/LiNbO₃ was examined. This process was considered to be usable for fabrication of LiNbO₃ optical waveguide devices with an Al thin film polarizer. However,

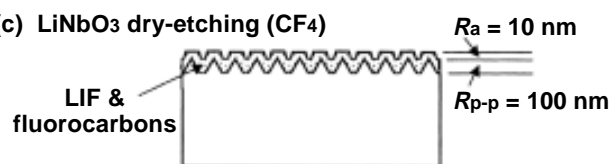
(a) SiO₂ film deposition



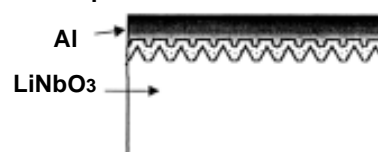
(b) SiO₂ dry-etching (CF₄)



(c) LiNbO₃ dry-etching (CF₄)



(d) Al film deposition



(e) Interface reaction



FIG. 10. Schematic depicting the process of Al film deposition on CF₄ plasma-etched SiO₂/LiNbO₃, causing Al film deterioration.

this process is not optimal, because the metallic nature of the resulting Al film was found to be deteriorated by the process. The main cause of the deterioration was a chemical reaction of the growing Al film with contaminants deposited on LiNbO₃ surface during the previous plasma etching.

ACKNOWLEDGEMENTS

This work is supported by Special Coordination Funds for Promoting Science and Technology "Fundamental Research on New Materials of Function-Harmonized Oxides," from the Japanese Science and Technology Agency.

REFERENCES

1. H. Nagata, T. Fujino, N. Mitsugi, and M. Tamai, *Thin Solid Films* **335**, 117 (1998).
2. H. Nagata, T. Shinriki, K. Shima, M. Tamai, and E.M. Haga, *J. Vac. Sci. Technol. A* **17**, 1018 (1999).
3. K. Noguchi, O. Mitomi, H. Miyazawa, and S. Seki, *J. Lightwave Technol.* **13**, 1164 (1995).
4. J.L. Jackel, R.E. Howard, E.L. Hu, and S.P. Lyman, *Appl. Phys. Lett.* **38**, 907 (1981).
5. K. Shima, N. Mitsugi, and H. Nagata, *J. Mater. Res.* **13**, 527 (1996).
6. H. Nagata, N. Mitsugi, K. Shima, M. Tamai, and E.M. Haga, *J. Cryst. Growth* **187**, 573 (1998).
7. N. Mitsugi, H. Nagata, K. Shima, and M. Tamai, *J. Vac. Sci. Technol. A* **16**, 2245 (1998).
8. Y. Suematsu, M. Hakuta, K. Furuya, K. Chiba, and R. Hasumi, *Appl. Phys. Lett.* **21**, 291 (1972).
9. H. Nagata, H. Takahashi, H. Takai, and T. Kougo, *Jpn. J. Appl. Phys.* **34**, 606 (1995).
10. H. Nagata, N. Mitsugi, T. Sakanoto, K. Shima, M. Tamai, and E.M. Haga, *J. Appl. Phys.* **86**, 6342 (1999).